Dynamic Nature of the Ligustilide Complex

Andreas Schinkovitz,[†] Samuel M. Pro,[‡] Matthew Main,[†] Shao-Nong Chen,[†] Birgit U. Jaki,[‡] David C. Lankin,[†] and Guido F. Pauli*[,†,‡]

UIC/NIH Center for Botanical Dietary Supplements Research and Program for Collaborative Research in the Pharmaceutical Sciences, Department of Medicinal Chemistry and Pharmacognosy, Institute for Tuberculosis Research, College of Pharmacy, University of Illinois at Chicago, Chicago, Illinois 60612

Received March 5, 2008

Monomeric phthalides such as *Z*-ligustilide (**1**) and *Z*-butylidenephthalide (**2**) are major constituents of medicinal plants of the Apiaceae family. While **1** has been associated with a variety of observed biological effects, it is also known for its instability and rapid chemical degradation. For the purpose of isolating pure **1** and **2**, a gentle and rapid two-step countercurrent isolation procedure was developed. From a supercritical CO_2 fluid extract of *Angelica sinensis* roots, the phthalides were isolated with high GC-MS purities of 99.4% for **1** and 98.9% for **2** and consistently lower qHNMR purities of 98.1% and 96.4%, respectively. Taking advantage of molarity-based qHNMR methodology, a time-resolved study of the dynamic changes and residual complexity of pure **1** was conducted. GC-MS and (qH)NMR analysis of artificially degraded **1** provided evidence for the phthalide degradation pathways and optimized storing conditions. Parallel qHNMR analysis led to the recognition of variations in time- and process-dependent sample purity and has impact on the overall assessment of time-dependent changes in complex natural products systems. The study underscores the importance of independent quantitative monitoring as a prerequisite for the biological evaluation of labile natural products such as monomeric phthalides.

The major phthalides 3-butylidene-4-5-dihydro-3*H*-isobenzofuran-1-one (*Z*-ligustilide, **1**) and 3-butylidene-3*H*-isobenzofuran-1-one (*Z*-butylidenephthalide, **2**) are common phytoconstituents of the Apiaceae.[1−4] Both phthalides have been shown to be associated with a variety of bioactivities such as vasodilative, antiatherosclerotic, and anticonvulsive effects.[5−8] Moreover, they are known to be unstable compounds.

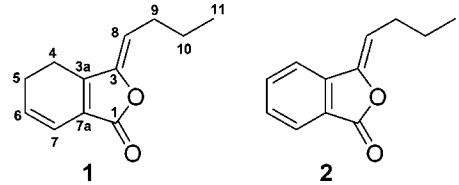

In order to establish links between an observed biological effect and the occurrence of specific phytochemicals, reference materials of the compounds have to be isolated from the natural material in sufficient quantity and purity. Solid phase-based chromatographic techniques experience irreversible binding of analytes to the stationary phase as well as limited loading capacities; therefore, several separation steps and copious solvent use is required to achieve a purified product. Demands arising from labile compounds such as **1** and **2** further complicate method development, as a long-lasting isolation procedure may severely decay those substances. One promising approach for the isolation of phthalides is the recently reported use of countercurrent separation (CS).[9,10] Keeping in mind both lability and target purity, the present investigation describes a rapid two-step CS-based isolation process that yields **1** and **2** in high-purity from crude plant extract. Concurrently, quantitative ^{1}H NMR (qHNMR) was developed to provide non-chromatographic evidence for the dynamic behavior of phthalide reference materials in terms of their composition and purity.

The isolation procedure utilizes a combination of fast centrifugal partition chromatography (FCPC) and high-speed countercurrent chromatography (HSCCC) for the preparative isolation of **1** and **2** from supercritical fluid extract of *Angelica sinensis* roots. Purity and stability of the isolates were simultaneously evaluated by GC-MS and qHNMR, which for the first time allowed for time-resolved observation of the dynamics and structural diversity of the degradation of **1**. The latter is of particular importance for phthalide reference materials such as **1**, which are well known to be unstable in the presence of light or oxygen[11,12] or kept in dry storage.[13] While previous studies have always employed chromatographic methods such as HPLC or GC-MS for stability evaluation, the perspective of qHNMR provides new insights into the dynamic phytochemistry of aging isolates of **1**.

A further goal of the study was to assemble a degradation pathway of **1** based on GC-MS, structural 1D/2D NMR, and qHNMR data of the artificial degradation of **1** and identify compounds that allow monitoring of the degradation of **1** in pharmaceutical preparations or herbal products. Because of the complex chemical degradation of **1**,[12] the study was designed to focus on compounds sufficiently volatile for GC analysis while masking the presumed photodimerization as an established pathway of phthalide degradation.[4,11] A final study goal was the development of storage conditions that minimize phthalide degradation and ensure long-term suitability of phthalide reference materials for biological and chemical studies.

Results and Discussion

Isolation Procedure and Purity Evaluation. Determining a suitable biphasic solvent system (SS) represents the most challenging task in CS and requires thoughtful attention. Applying a recent publication,[14] TLC experiments suggested that mixtures of *n*-hexanes, EtOAc, MeOH, and water, referred to as the HEMWat SS family in the literature,[14,15] are a suitable SS for the purification of **1** and **2**. In subsequent CS experiments, HEMWat −7 (9:1:9:1, v:v) produced superior separations. UV profiles of FCPC and HSCCC experiments are shown in Figure 1. Target compound **1** is associated with peaks between 60 and 85 min (K = 2.57; all calculations follow Gaussian peak shapes) in the first FCPC and 215−271 min (K = 2.27) in the second HSCCC isolation step, respectively.

* To whom correspondence should be addressed. Tel: (312) 355-1949. Fax: (312) 355-2693. E-mail: gfp@uic.edu.
† UIC/NIH Botanical Center and PCRPS.
‡ Institute for Tuberculosis Research.

10.1021/np800137n CCC: $40.75
Published on Web 09/10/2008

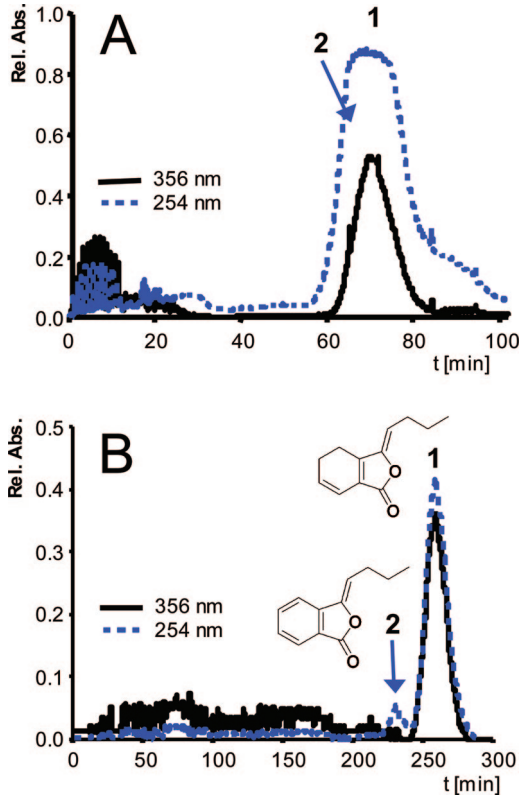

Figure 1. UV chromatograms (time plots, 254 and 365 nm) of the two-step liquid−liquid isolation procedure used to resolve *Z*-ligustilide (**1**) from *Z*-butylidenephthalide (**2**). The first step (A) employed centrifugal partition chromatography (CPC, V_{tot} = 1000 mL, HEMWat −7 solvent system, S_f = 64%) and can accommodate injection of crude plant extract to achieve significant enrichment of the monomeric phthalides. While **1** and **2** remain largely coeluting entities, their full resolution is achieved in step B by high-speed countercurrent (HSCCC, V_{tot} = 120 mL triple-coil J-type centrifuge, HEMWat −7, S_f = 76%) to yield both **1** and **2** in high purity as established by qHNMR and GC-MS analysis (see discussion).

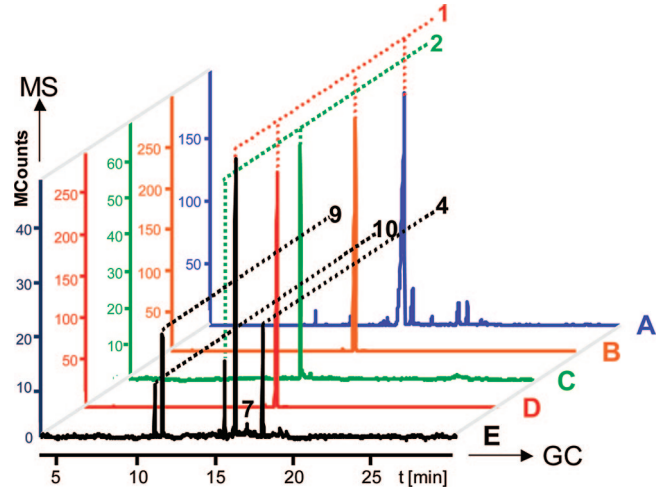

Figure 2. GC-MS profiles of phthalide-containing materials in various stages of purification and degradation of the monomeric phthalides **1** (*m/z* 190, t_R 15.784 min) and **2** (*m/z* 188, t_R 15.004 min): A = crude SFE extract of *A. sinensis*; B = fraction enriched with **1** after the first purification step (Figure 1A); C = **2** isolated from B; D = **1** isolated from B; E = sample of pure **1** after 4.5 h of degradation in the dry state at 4 °C. Peaks of structurally assigned degradation products are 3,8-epoxiligustilide (**4**, *m/z* 206, t_R 19.576 min), senkyunolide D (**7**), 2,3-dihydrophthalic acid anhydride (**8**, *m/z* 150, t_R 12.234 min), and phthalic acid anhydride (**10**, *m/z* 148, t_R 10.356 min).

In order to assess the separation efficiency of a single-step CS isolation procedure, the primary FCPC (V_{tot} = 185 mL) fractions were analyzed by TLC, GC-MS, and NMR. Normal-phase TLC focused on a single spot at R_f 0.66 from fraction K = 2.57, with $CHCl_3$ as mobile phase. This spot showed strong fluorescence under 356 nm UV and turned to a blue-gray hue after development with vanillin−H_2SO_4 reagent. GC analysis revealed the presence of two compounds, a minor one eluting at 15.050 min and a predominant one eluting at 16.131 min. These compounds were identified as **2** and **1** by comparing their MS fragmentation pattern as well as ^1H and ^{13}C NMR spectra with previously published data.[17−19] The highest purity of **1** achievable from primary CS fractionation was 97.9%, as determined by GC-MS, and required recombination of the fractions eluting between 60 and 75 min (K = 2.46). The only GC-detectable impurity was **2**, which on the basis of TIC integrals amounted to 2.1% (Figure 2B). This is in contrast to the qHNMR analysis, which resulted in a measured purity of 83.0% for the same sample. Utilizing the 100% qHNMR method,[20−22] which avoids the uncertainty of widely varying GC response factors, the amount of **2** was determined to be 8.8%. At the same time, 8.2% of additional unidentified impurities were found to be present. These results clearly indicated that further purification is necessary to obtain reference material with adequate purity for biological evaluation.

The combined FCPC fraction (K = 2.46) was subjected to secondary HSCCC fractionation (V_{tot} = 120 mL). Although the same SS was used, **1** and **2** were now readily separated as indicated by UV traces (Figure 1B): The aromatic **2** eluted before the olefinic **1**, between 215 and 239 min (K = 2.10) and was observed at UV 256 nm. The highest purity for **2** (98.9% by GC-MS, Figure 2C; 96.4% by qHNMR, 0.5 mg from 140.1 mg of SFE extract) was achieved by recombining elution volumes between 215 and 229 min (K = 2.04). Target compound **1** eluted between 236 and 271 min (K = 2.38), producing a major symmetrical peak in the UV at 256 and 356 nm. Recombined fractions collected between 241 and 247 min (K = 2.28) showed the highest purity for **1** of 99.4% by GC-MS (Figure 2D) and 98.9% by qHNMR. On the basis of crude plant material, the overall yield of this two-step process was 8.5% for the main target compound **1** (11.9 mg from 140.1 mg of SFE extract) and 0.4% for the minor compound **2**.

The contemporary CS literature contains an increasing number of reports on the suitability of single-step CS procedures for the isolation of highly pure reference materials from crude extracts, which indicates high selectivity of the CS process.[23] While the present study was under way, Zhang et al.[10] reported a one-step HSCCC isolation procedure that utilized a different SS (HEMWat + MeCN, 8:2:5:5:3) and yielded **1** with a GC-FID purity of 98.0%. In order to evaluate the influence of MeCN as a selectivity modifier of HEMWat SSs and verify the need for the labor-intensive two-step isolation procedure, the one-step method was reproduced on a comparable 320 mL HSCCC instrument. As expected, the elution of **1** was shifted to higher K values due to the addition of MeCN, which made the aqueous phase more lipophilic compared to the HEMWat SS. Despite the commonly found resolution advantage of an upper K working range ($1 < K < 4$), the separation efficiency was not significantly better than during the primary FCPC fractionation. In fact, after combining the analogous fractions between 489 and 510 min (K = 3.65), the GC-MS purity was only 94.7%. This value was still lower than the 98.0% reported GC/FID purity and the observed 98.9% GC-MS purity from the primary FCPC separation.

The apparent 2.6-fold deviation in the amount of impurities in the reported[10] versus the reproduced CS method is reasonably explained by different response factors *between two detection*

methods, FID and MS. Aside from this obvious source of error in purity analysis, significant differences in response factors also have to be considered *within the same detection method*. This was clarified by subsequent qHNMR analysis, which again revealed a lower degree of purity at 83.2% for **1**. Interestingly, this was essentially identical with the 83.0% qHNMR purity observed after the present primary CPC step and indicated that MeCN did not improve the selectivity of the SS. The considerable difference between GC-MS and qHNMR purity assessments is not necessarily a contradiction and can be attributed to various factors. In GC-MS, not all impurities are volatile (e.g., phthalide dimers) or undergo efficient ionization in the mass spectrometer, and largely variable response factors have been taken into consideration.[24,25] However, qHNMR is not affected by these factors; it is independent of ionization rates and analyte volatility. Moreover, qHNMR indicates the presence of any impurity that contains hydrogen atoms, and signal integrals have a linear, straight molarity-based correlation with analyte concentration. Finally, it is a nondestructive method of analysis.[22]

Stability Evaluation of 1. Several reports have described **1** as a compound of low chemical stability with a high propensity for reactions involving oxidation and dimerization.[11−13,26] As **1** has been implicated in various bioactivities,[5−8] methods for monitoring stability and establishing conditions for long-term storage are of critical importance for pharmaceutical and herbal preparations. In the course of this study, the stability of **1** was examined when stored at −30 °C in organic solvents such as hexane-d_{14}, MeOH-d_4, DMSO-d_6, $CDCl_3$, and HEMWat −7 upper phase by qHNMR and, concurrently, by GC-MS for the solvents *n*-hexanes, $CHCl_3$, and HEMWat −7. HEMWat −7 test samples were dried under argon and redissolved in $CDCl_3$ instantly before qHNMR evaluation. The results of the qHNMR and GC-MS analyses are summarized in Figure 3. The qHNMR experiments indicate that **1** is most stable when stored in HEMWat −7 upper phase, which represents the mobile phase of the two isolation steps. In a period of 41 days, the level of **1** decreased by only 0.8%. This is convenient since fractions from the isolation procedure can be stored without further processing. Stability was also found for **1** when stored in deuterated DMSO or MeOH, showing a mild decrease of 5.2% and 4.4%, respectively, after 41 days. The fact that DMSO is solid at −30 °C did not impair its preservative effect on **1**. The $CDCl_3$ sample of **1** showed the lowest stability with a decrease of 15.6% within the 41-day period. This result is not surprising, since $CDCl_3$ when exposed to light is known to degrade, producing HCl and phosgene, both of which are agents that can promote degradation of **1**.[27] Due to overlapping signals of **1**, hexane-d_{14} was not a suitable solvent for qHNMR analysis of **1**.

GC-MS analysis showed a steady decline in the concentration of **1** when stored in hexane (5.9%) or $CHCl_3$ (2.3%) over a period of 46 days. Confirming what was already observed during the purity evaluation of **1** and **2**, qHNMR and GC-MS data exhibited different results with respect to the stability evaluation. While the $CDCl_3$ sample, which had been aged for 46 days, still showed the presence of 91.6% of **1** remaining by GC, qHNMR showed only 78.1% present. This deviation may be due to the differences in the content of HCl and/or phosgene in the solvents, $CHCl_3$ versus $CDCl_3$, used for GC and NMR experiments, respectively. To resolve this ambiguity, the qHNMR sample was also analyzed by GC-MS. The results still gave the content of 96.1% of **1** in the sample.

Two reports have independently examined the stability of **1** in solution. Cui et al. described the stabilizing influence of added antioxidants such as ascorbic acid in combination with propylene glycol and glycerol on **1**.[12] Zhou and Li investigated the solvent effects of cyclohexane and $CHCl_3$ on the stability of **1** by GC-MS, thus complimenting our results.[13] This study also found the stabilizing effect of $CHCl_3$ on **1** when monitored by GC-MS. However, no concurrent qHNMR analysis was performed in this study.

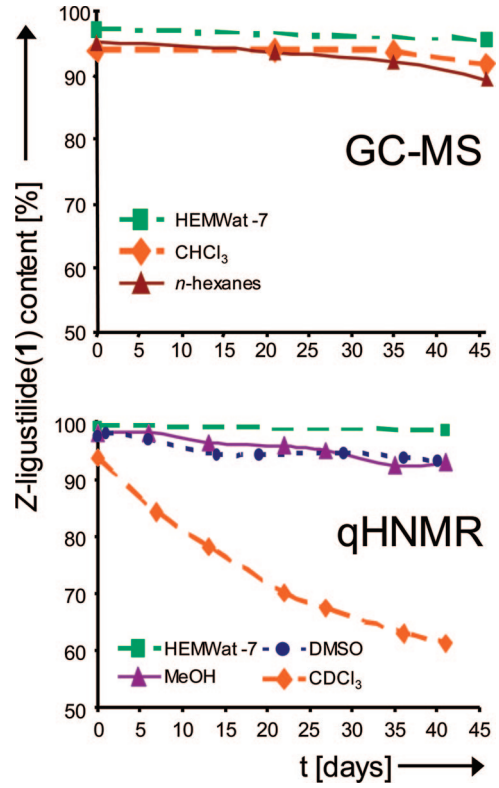

Figure 3. Determination of the midterm stability of **1** in four typically used neat organic solvents (MeOH, DMSO, $CDCl_3$, *n*-hexanes) and the multicomponent CCC solvent system (SS; HEMWat −7) at 1 mg/mL, as determined by GC-MS (top) and qHNMR (bottom). While being most stable in the CCC SS, degradation of **1** in neat solutions of MeOH and DMSO occurs in a quasi-linear fashion at a rate of ∼4% per month. The instability of **1** in $CHCl_3$ solution with a ∼40% loss over 1.5 months, which required qHNMR for detection, underlines the critical choice of the analytical method used for (im)purity profiling of natural products in general.[38] Compared with chromatographic methods, qHNMR is significantly more universal in detecting degradation, mostly by virtue of the lack of response factors and due to the ubiquitous presence of protons in the degradation products.

Forced Degradation of 1. Degradation in the amount of 15% was observed by GC-MS, when dried **1** was stored at −30 °C for 24 h (data not shown), suggesting that the actual decay is much higher when analyzed by qHNMR. To study this phenomenon in a time-resolved fashion, **1** was dried by a stream of argon and stored in the dark at 4 °C for 3, 6, 9, 12, 18, 24, 29, 36, and 42 h before being redissolved and analyzed. Artificial degradation could be used to determine marker compounds as potential indicators of the degradation processes associated with **1** in pharmaceutical or herbal preparations. Unfortunately, additional overlapping of the signals in the 400 MHz ^{1}H NMR spectra, particularly in the high-field aliphatic region, significantly complicated the spectra and limited the qHNMR approach for purity evaluation. In this respect, the GC-MS data were less complex, as degradation products were better separated from one another in the chromatogram. For this reason, five degradation products that are clearly distinguishable in the GC-MS chromatogram were chosen (see Figure 2E) as markers to monitor the degradation processes associated with **1**. Their masses appear at *m*/*z* 148, 150, 188, 206, and 222. It is worth noting that none of these signals except *m*/*z* 188 were observed during the stability evaluation of **1**, confirming that its decay is much delayed in solution and concentrations of some degradation products are

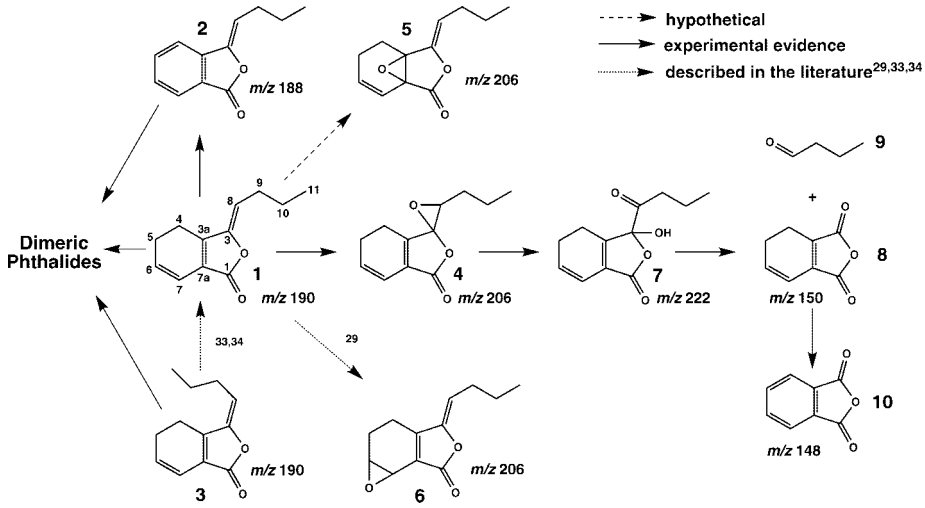

Figure 4. Proposed degradation pathway of **1** summarizing present GC-MS and NMR experimental evidence as well as literature knowledge (see discussion) and involving the following compounds: *Z*-ligustilide (**1**) *Z*-butylidenephthalide (**2**), *E*-ligustilide (**3**), 3,8-epoxyligustilide (**4**), 3a,7a-epoxyligustilide (**5**) unlikely side product, 6,7-epoxyligustilide (**6**), senkyunolide D (**7**), 4,5 dihydro-1,3-isobenzofuranon (**8**), butyraldehyde (**9**), and phthalic acid anhydride (**10**).

beyond the threshold of detection. Dimerization of **1** linked to degradation has been previously described by Quiroz-Garcia et al.[11] but will be excluded from consideration, as dimers could not be detected by GC-MS.

The peak associated with *m*/*z* 190 represents residual **1**. The MS-based structural information was used to mutually guide the interpretation of qualitative 1D and 2D ^{1}H NMR experiments.

A proposed degradation pathway underlying combined GC-MS and NMR evidence is outlined in Figure 4. On the basis of GC-MS analysis, the formation of **2** (*m*/*z* 188) was indicated by both the observed retention time and the fragmentation pattern, in reference to previously isolated **2**. Further support comes from the ^{1}H NMR spectrum. Although many regions of the spectrum were complex and overlapped, the following key signals clearly related to **2** could be identified: a triplet at δ 5.642 (1H, J = 8.0, H-8) together with the aromatic signals of H-6 (δ 7.509, 1H, ddd, J = 7.7, 7.3, 0.9), H-4 (δ 7.661, 1H, ddd, J = 7.8, 0.9, 0.8), and H-5 (δ 7.680, 1H, ddd, J = 7.8, 7.3, 1.0). Assembling the chemical shift, splitting pattern, and integral information provided clear evidence for the formation of **2**. The aromatic signal of H-7 at δ 7.895 overlapped with an additional signal linked to another degradation product of **1**, phthalic acid anhydride (**10**). Its molecular ion at *m*/*z* 148 (Figure 4) and MS fragmentation pattern were consistent with previously published data.[28] The ^{1}H NMR spectrum showed the characteristic resonances of the AA′XX′ spin system that give rise to two symmetrical signals at δ 8.033 and 7.919. As noted earlier, the AA′XX′ signal at δ 7.919 overlaps with one of the aromatic signals (δ 7.896) of **2**, so its splitting substructure cannot be analyzed completely. Nevertheless, the AA′XX′ signal at δ 8.033 fully matched the spectrum of authentic reference material of **10**. In consecutive selective 1D SelTOCSY experiments, excitation of the signal at δ 8.033 resulted in production of a single "correlation" signal at δ 7.919, further supporting the presence of **10** and absence of further spin-connected partial structures. GC chromatograms of authentic **10** and a degraded sample of **1** showed corresponding peaks of **10** at 10.366 min (±0.020 min, depending on concentration) with identical MS fragmentation patterns.

A further degradation product of **1**, compound **8**, exhibited its molecular ion at *m*/*z* 150 and was identified as a dihydrogenated derivative of **10**. This assignment is supported by the homologous MS fragmentation sequence: initial elimination of CO_2 (−44 amu→ *m*/*z* 104 in **10**, *m*/*z* 106 in **8**), followed by subsequent loss of CO (−28 amu → *m*/*z* 76 in **10**, *m*/*z* 78 in **8**) and retro Diels−Alder ring cleavage to yield a mass fragment at *m*/*z* 50 in both **10** and **8**. While the exact homology of the fragments prior to ring cleavage indicates that one of the aromatic double-bond equivalents of **10** has been saturated to yield **8**, the position of dihydrogenation could not be verified by GC-MS. Considering that **8** is a direct degradation product of **1**, a shift of unsaturation is unlikely and the evidence is best compatible with the structure of 4,5-dihydro-1,3-isobenzofuranon (**8**). This compound was found to be an early, metastable species in the dynamic mixture of degradation products. Its GC peak diminished over time, whereas the peak area of **10** increased, indicating that **8** is likely converted into **10**, possibly by a disproportionation mechanism where one of two molecules **8** is reduced to the dehydro form (not detected) and the other oxidized to **10** (anhydro form, detected), analogous to the conversion of **1** to **2**.

Another GC-prominent degradation product of **1** exhibited a molecular ion at *m*/*z* 206, suggesting a structure in which either an epoxidation of one of the double bonds or introduction of an OH group accompanied by the elimination of an H atom has occurred. The epoxidation leaves further room for speculation, as any of the three double bonds of **1** could be potentially affected (Figure 4: 3,8-epoxyligustilide [**4**], 3a,7a-epoxyligustilide [**5**], 6,7-epoxyligustilide [**6**]). The existence of compound **5** has not been previously reported, and our experiments did not show any hint of its existence. Isomer **6**, 6,7-epoxyligustilide, has previously been reported from the rhizome of *Ligusticum wallichii* and linked to the degradation of **1**.[29] In this report, the ^{1}H NMR shifts of the epoxidized protons at C-6 and C-7 were observed at δ 4.33 and 4.61, respectively, but none of these specific proton signals were present in our spectra of degraded **1**, which eliminated structure **6** from consideration. Similar to compound **5**, the isolation of **4** has not been previously reported. Like degradation product **8**, the designated epoxide (*m*/*z* 206) is unstable, which leaves the GS-MS profile as the primary source of structural information. In the context of an interconnected degradation complex, epoxidation of the C-3/C-8 double bond appears to be most likely. Formation of **8** requires a dehydrogenation of the double bond and a cleavage of the aliphatic side chain present in **1**. This may be facilitated by the transformation of the epoxide into a glycol and further into senkyunolide D (**7**), a compound that has been reported by Kobayashi et al. (Figure 4).[30] Compound **7** exhibits a molecular ion at *m*/*z* 222, which can also be observed in the GC-MS chromatogram of degraded **1**. This species may act as an intermediate prior to the cleavage of the C-3/C-8 σ-bond, which would result in the formation of **8** and *n*-butyraldehyde (**9**). Support for this hypothesis came from the occurrence of the characteristic

^{1}H NMR fingerprint of **9** in degraded **1**: a triplet for the aldehyde proton at δ 9.772 ($J = 1.7$) and a sextet at δ 1.684 ($J = 7.4$), linked to the α-carbonyl protons by COSY correlations. This is in full agreement with data acquired from reference material and with published NMR data for **9**.[32] Interestingly, **9** has been reversibly used to introduce the aliphatic side chain to a lactone body during the synthesis of **1**.[31]

The presence of the precursor epoxide **4** is supported by the observation of a doublet of doublets ($J = 6.8, 5.4$) at δ 3.396, indicating an oxymethine proton attached to the C-8 position. It is shifted almost 2 ppm upfield compared to the proton linked to C-8 in **1**. This shift can reasonably be caused by the epoxidation of the double bond between C-3/C-8. A consecutive HSQC spectrum exhibited a cross-peak between the observed ^{1}H signal at δ 3.396 and its corresponding C at δ 61.82, further supporting the presence of an epoxide between position 3 and 8. Next an HMBC experiment revealed the predictable cross peak to C-9 of the aliphatic at δ 29.85, but not to the quaternary C-3a (expected at δ ~90). Considering the low concentration of **4** and the limiting factor of a disadvantageous dihedral angle, this observation is expected.

A selective 1D TOCSY (1D SelTOCSY, τ_{mix} 80 ms) experiment exciting the proton at δ 3.396 revealed three aliphatic signals at δ 1.873 (m), 1.554 (m), and 0.997 (t, $J = 7.4$ Hz) belonging to the same spin system. The signals at δ 1.873 and 1.564 are associated with the methylene protons at C-9 and C-10, respectively. Their coupling pattern is complex and can be explained by the magnetic nonequivalence of the participating H atoms due to the strong anisotropic influence of the epoxide group. The 3H signal at δ 0.997 of the terminal Me appears as a sharp triplet, because it is already four bonds away from the epoxy group. Finally, literature-based prediction of ^{1}H and ^{13}C chemical shifts of **4** (ACD/NMR databases) seamlessly matched with the observed chemical shifts of the aliphatic side chain in the HSQC, HMBC, and 1D SelTOCSY experiments and corroborated the structural assignment: C-8 63.99/61.82, H-8 3.40/3.396; C-9 31.30/29.85, H-9 1.71/1.867; H-10: 1.556/1.554; H-11 0.97/0.997 [δ(predicted)/δ(observed)]. As noted earlier, **4** as well as **7** and **8** are transient "metastable" degradation intermediates. Their concentrations increase and diminish within a few hours of the degradation process; therefore, it is more than questionable whether it is possible to isolate those intermediates for complete conformation of their proposed structure.

GC-MS and NMR Monitoring of the Dynamic Degradation Processes. Both techniques have advantages and limitations. GC-MS offers a quick method to detect specific degradation products; however, not all impurities will be detected. Notably, when dealing with highly purified phthalides, GC-MS may not reflect the current status of degradation. Quantitative ^{1}H NMR is capable of detecting impurities or degradation products that contain protons with typical detection limits of 0.1%, or below. As a sample like **1** progressively degrades, the qualitative and quantitative interpretation of the qHNMR spectra becomes an increasing challenge due to increasing peak overlap, especially in the high-field aliphatic region. As a result, individual species within overlapping signal groups become more difficult to distinguish and to quantify. In order to overcome this problem, 1D and 2D NMR experiments (such as COSY and 1D SelTOCSY used in this study) can be performed to verify signal assignments and assemble groups of signals that belong to the same molecular species.

It is feasible to identify structural markers that are associated with the degradation processes by qHNMR alone or in combination with GC-MS. In the case of **1**, GC-MS analysis led to the assignment of **2** (*m/z* 188), **4** (*m/z* 206), **8** (*m/z* 150), and **10** (*m/z* 148) as the four most prominent degradation products. However, using qHNMR allowed for the monitoring of the degradation process as shown in Figures 5 and 6. When their intensity is correlated over time (time-resolved), the signals also represent dynamic markers for the degradation process. Key signals associated with specific compounds such as **2** and **10** are well separated and can be directly detected, although the overall concentration of the

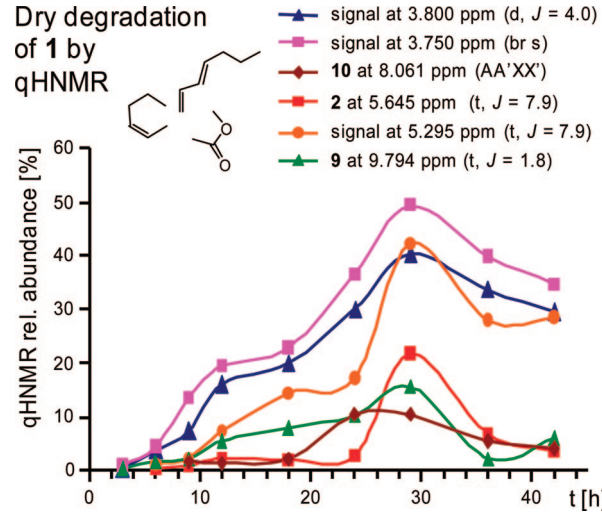

Figure 5. Selected qHNMR indicators for the degradation of **1** in dry stage at +4 °C. Signals associated with degradation products were primarily chosen due to their isolated position in otherwise crowed spectra. Some of them can be linked to specific compounds, such as the degradation products **2**, **9**, and **10**. The reference signal for quantitation was the signal of proton H-6 (1H, dt, $J = 9.6, 4.2$) of **1** at δ 6.005. Its integral was set to 100%, and the % quantities of the degradation products were calculated from their integral values in relation to this reference. All observed degradation signals increased in intensity for 29 h after the beginning of degradation of **1**. Thereafter, signal intensities steadily declined, which indicates that qHNMR-observable degradation products might not be the end point of the decay of **1**. This is supported by the observation that the increase of strongly overlapping signals in the range δ 0.8−2.9 is also transient and that curves for the time course of this aliphatic material follow a similar trend. Thus, it is reasonable to believe that qHNMR-transparent and/or volatile species such as CO_2 are among the ultimate degradation products of **1**.

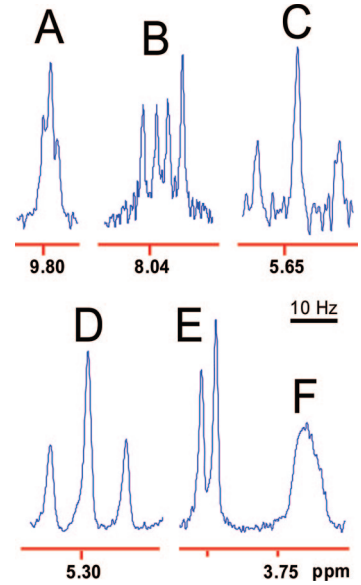

Figure 6. Characteristic qHNMR signals of key degradation products of **1** in dry state at +4 °C. A: butyraldehyde (**9**, δ 9.795, 1H, t, $J = 1.7$); B: phthalic acid anhydride (**10**, δ 8.033, AA′XX′, 2H, $J = 7.8, 2.1, 0.8$); C: *Z*-butylidenephthalide (**10**, δ 5.642, 1H, t, $J = 8.0$, H-8); D: unknown butylidene derivative (**2**, δ 5.295, 1H, t, $J = 7.9$ Hz); E: unknown compound (δ 3.800, 1H, d, $J = 4.0$ Hz); G: unknown compound (δ 3.750, 1H, br s/m).

latter compounds remains low. More prominent signals such as a 7.9 Hz triplet centered at δ 5.295, a 4.0 Hz doublet at δ 3.800, and a broad singlet at δ 3.750 can be found in the spectrum of degraded **1**. These signals are also well separated from crowded areas of the ^{1}H NMR spectrum and represent solid markers of the degradation process. At this point, no specific structure can be associated with these signals, but some assumptions concerning structure fragments can be inferred. Selective 1-D TOCSY excitation of the triplet at δ 5.295 showed the same correlation and splitting pattern as the excitation of H-8 in **1**, proving the existence of the same aliphatic side chain. *E*-Ligustilide (**3**) has a downfield shifted H-8 proton,[33] but its formation could be ruled out as **3** was reported to quickly transform into **1** and not vice versa [33,34] and no additional peak at *m*/*z* 190 could be observed by GC-MS. Considering these findings, present results indicate that the signal observed at δ 5.295 could potentially belong to a dimer; although based on the limited information available, no correlation to NMR data for previously published dimers was found.[11,18,26] As mentioned earlier, dimer formation has been described for **1** particularly when exposed to light;[11] all reported experiments, however, were carried out in the dark.

To assign the signals centered at δ 3.800 (d, $J = 4.0$) and 3.750 (br s/m), a 1D SelTOCSY (τ_{mix} 80 ms) was employed, which indicated mutual coupling of these signals. While this explains the 4 Hz splitting in the signals at δ 3.800, the experiment was unable to link the signal at δ 3.750 to other signals of what must be a spin system with long-range correlations, as indicated by the fine multiplet splitting of the signal at δ 3.750.

Figure 5 visualizes the dynamic nature of the degradation of **1** by monitoring the key signals at δ 3.750 (br s/m, unknown compound), 3.800 (d, $J = 4.0$, unknown compound), 5.295 (t, $J = 7.9$, unknown compound), 5.645 (t, $J = 7.9$, **2**), 8.061 (AA′XX, **10**), and 9.772 (t, $J = 1.7$, **9**). A steady increase of all integrated signal intensities could be observed during the first 29 h, before all signals would exhibit an unexpected but steady decrease. Proton C-6 of **1** (δ 6.005, 1H, dt, $J = 9.6, 4.2$) was selected as the reference signal (100%) for the qHNMR analysis because it remained well isolated from all other signals that occurred during the degradation process. Figure 5 also confirms the observation made during the 1D SelTOCSY experiment for correlating signals at δ 3.750 (br s) and 3.800 (d, $J = 4.0$). A plot of their signal intensities as a function of time shows a parallel course, confirming that they both belong to the same unknown compound. A rapid increase in the signal intensities in the high-field region of the spectrum (δ 0.8−2.9) indicated one possible end point of the degradation. These signals are not outlined in Figure 5, because they are overlapped with one another, rendering subsequent detailed analysis impossible. It is important to note that the increase of overlapping signals in the range δ 0−2.9 is also transient and that time curves of this aliphatic material follow a trend similar to that of degradation intermediates. One possible explanation for the apparent loss of qHNMR-accountable integral/signal intensity is that the ultimate degradation products of **1** are ^{1}H NMR-transparent or volatile species such as CO_2.

Conclusions. By applying a two-step FCPC- and HSCCC-based isolation scheme, **1** and **2** can be purified from the supercritical fluid extract of *A. sinensis* roots in high yield and high chemical purity. Compound **1** was found to be most stable when stored in solution in the mobile phase (HEMWat −7, upper phase) at −30 °C. The results further demonstrate that the purity and stability evaluations of **1** require the use of qHNMR as a valuable adjunct to GC-MS alone. Because the latter may not reveal all of the impurities or degradation products, qHNMR demonstrated a significant advantage in providing an accurate quantitative assessment of phthalide reference materials.

For the elucidation of the dynamic degradation process, the combined use of GC-MS with qHNMR in artificial degradation studies was most efficient. Apart from storing **1** in the upper phase of HEMWat −7 as the best stabilizing agent, other organic solvents such as MeOH and DMSO can also preserve **1**. This observation is of specific importance for bioassays where DMSO solutions are widely used. The preservative effect of organic solvents does not hold true for $CDCl_3$, where **1** exhibited significant degradation over a short time period. Degradation of **1** shows the formation of **10** and **2**, both of which can be monitored by GC-MS and qHNMR. The presence of **10** represents a good marker compound for the stability evaluation of **1** contained in herbal or pharmaceutical preparations, because **10** has not previously been reported as a natural plant ingredient.

On the basis of the results presented here, handling of **1** demands special precautions for its isolation, purity evaluation, and preservation. Furthermore, the degradation processes can impart significant changes in the observed bioactivities and should be addressed by specifically modified bioassays and evaluation techniques. A parallel report focusing on the important aspect of degraded **1** in the induction of quinone reductase appears separately.[35] A recently published report that describes an investigation of the pharmacokinetics and metabolism of **1** elucidates metabolomic products partially identical with those formed in the degradation process of **1**.[36] Without doubt, **1** represents a case of a particularly unstable naturally occurring compound and exemplifies the importance of monitoring time-dependent changes of an already complex natural products system prior to drawing conclusions about its observed biological function.

Experimental Section

General Experimental Procedures. UV chromatograms were recorded by a preparative flow cell UV detector (Shimadzu, Columbia, MD) during the isolation procedure of **1** and **2** at set wavelengths of 254 and 356 nm. Proton NMR experiments (δ in ppm, J in Hz) for structure elucidation and purity evaluation were performed on a Bruker DPX-400 spectrometer (Karlsruhe, Germany), using standard proton acquisition programs. Spectral width (SW) was 11.968 ppm, and the shift of the center of the spectrum (O1P) was 5.500 ppm. Acquisition time (AQ) was set to 6.84 s, pulse width (PW) was 12.00 μs, 256 scans were performed, and relaxation delay (D1) was 1.00 s. The ^{13}C acquisition parameters were as follows: SW: 240.05 ppm, O1P: 110 0.00 ppm, AQ: 1.35 s, D1: 1.00 s. NMR tubes (S-5-400-7) were purchased from Norell Inc., Landisville, NJ. The NMR data were processed using the NUTS software package (Acorn NMR Inc., Livermore, CA). The qHNMR processing parameters were set as follows: line broadening factor −0.3, Lorentzian/Gaussian factor 0.05, triple zero filling prior to Fourier transformation. NMR spectra simulations were performed on ACD/SpecManager software (Advance Chemistry Development, Inc., Toronto, Ontario, Canada). Selective TOCSY experiments for the structure elucidation of degradation products of **1** were performed on a Bruker ADVANCE-400 spectrometer (Karlsruhe, Germany). Soft pulse excitation was applied to the following set points: 3.403, 5.315, and 8.056 ppm. SW was set to 11.9680 ppm, PW was 13.20 μs, and 2000 scans were performed for each experiment. Digital resolution was better than 0.0004 and 0.008 ppm for ^{1}H and ^{13}C, respectively, and chemical shifts are reported with three and two decimal places on the ppm scale, respectively, to appropriately reflect relative chemical shifts of signals.

The GC-MS experiments were carried out on a Varian CP-3800 gas chromatograph (Varian Inc., Lake Forest, CA) attached to a Varian 1200 Quadrupole MS and a Varian CP 8400a auto sampler. GC-MS conditions were as follows: column: VF-5 ms (Varian) capillary column (5% phenyl-, 95% dimethyl polysiloxanes), length: 30 m, 0.25 mm i.d., film thickness: 0.25 μm, carrier gas: helium ultrapure carrier grade (Airgas Inc.), flow rate: 1.0 mL/min, sample injection volume: 1 μL, no split, injector temperature: 250 °C, temperature program: 50 °C, increasing 10 °C/min up to 250 °C, then kept at this level for 10 min. MS conditions: electron impact (EI) ionization at 70 keV, scan range *m*/*z* 50−650, solvent acquisition delay 3.0 min.

Supercritical fluid extraction (SFE) of ground root material was performed on a Spe-ed SFE extraction device (Applied Separation Inc. Allentown, PA) consisting of a column oven, an air pressure regulator, and a 160 mm × 15 mm i.d. stainless steel extraction column attached

to a NESLAB RTE 7 refrigerated bath (Thermo Electron Corporation, Waltham, MA). Compressed air (dry grade) and CO_2 were purchased from Airgas Inc., Radnor, PA. The extraction column was filled with 46 g of ground plant material. Glass wool inserts were used to protect the frits at each end of the column. Extraction temperature was set to 40 °C. Prior to extraction, the filled column was allowed to rest for 15 min in the column oven in order to adapt to the temperature. Extraction was performed at 3800 psi for 7 min. The supercritical fluid extract was collected into a glass vial for 2 min. In order to preserve the stability of **1**,[37] the extract was immediately dissolved in a mixture of upper and lower phases of the solvent system used in the subsequent FCPC experiment. This procedure was repeated twice in order to process 138 g of plant material.

Fast centrifugal partition chromatography (FCPC) experiments were performed on a fast centrifugal partition chromatograph (CPC; Kromaton, Angers, France) equipped with a 185 mL rotor and a 10 mL sample loop. The system was attached to a digital single piston solvent pump (LabAlliance, State College, PA) and a sample collector (Labequip, Markham, Ontario, Canada). The solvent system hexane (Hex)/ethyl acetate (EtOAc)/methanol (MeOH)/H_2O (9:1:9:1, v/v) (HEMWat −7) was prepared in a separation funnel. After intense mixing, the two phases were allowed to separate for 1 h before being separated into different glass bottles. The hex/EtOAc-dominated upper phase was used as the mobile phase, and the MeOH/H_2O-dominated lower phase as the stationary phase (tail to head). The stationary phase was pumped into the device at a flow rate of 5 mL/min (no spin), which was maintained throughout the experiment. The column rotor was accelerated to a rotation speed of 1300 rpm prior to introduction of mobile phase. After achieving equilibrium the stationary phase retention (S_F) was calculated (64%) at a system pressure of 600 psi. During the entirety of the experiment, the flow rate was 5 mL/min and fractions were collected every 60 s.

High-speed countercurrent chromatography (HSCCC) was performed on a J-type high-speed countercurrent chromatograph (model CCC-1000 Pharma Tech Research Co., Baltimore, MD) containing a self-balancing three-coil centrifuge equipped with 3 × 40 mL or 3 × 108 mL coils. Coils were wrapped with PTFE tubing (1.6 mm i.d.) The revolution radius of the distance between the holder axis and the central axis of the centrifuge (R) was 7.5 cm. The β ratio (β_r) varied from 0.47 at the internal terminal to 0.73 at the external terminal (where $\beta_r = r/R$, where r is the spool radius and R represents the rotor radius). Sample loop size was 2 mL. The system was attached to a LabAlliance digital single piston pump for solvent delivery and an ISCO Foxy Jr fraction collector. The same solvent system and the same conditions mentioned in the preceding paragraph were applied with two exceptions: first, rotation speed was set to 1200 rpm and, second, flow rate was 1.0 mL/min. S_F was determined to be 74% and the system pressure was 90 psi after equilibration. The flow rate was maintained at 1.0 mL/min during the experiments and fractions were collected every 90 s.

Thin-layer chromatography (TLC) was performed with a focus on two specific objectives: (A) optimize the two-phase solvent system for consecutive FCPC and HSCCC experiments following a procedure previously described in the literature[14] and (B) monitor the fractions collected from FCPC and HSCCC experiments in order to decide which of those could be recombined. Chloroform was used as a solvent system for this purpose.

All TLC experiments were carried out on analytical silica gel 60 plates (ALUGRAM SIL G/UV_{254}, Macherey-Nagel, Düren, Germany). For chromatogram detection, TLC plates were observed under UV_{354} and sprayed with vanillin-H_2SO_4 reagent. The latter was prepared by dissolving 0.8 g of vanillin in 76 g of nondenaturized EtOH and 4 g of concentrated H_2SO_4. After spraying with the reagent, the plates were developed under a hot air stream (heat gun) for approximately 2 min.

Organic solvents except nondenatured EtOH used during the isolation process and TLC experiments were all obtained from Fisher Scientific, Hanover Park, IL, and distilled before use. Water (H_2O) was obtained from a Milli-Q water purification system (Millipore, Molsheim, France). Nondenatured EtOH was purchased from Aaper Alcohol and Chemical Co., Shelbyville, KY. Concentrated H_2SO_4 and reference substance **10** (99% analytical grade) were obtained from Sigma Chemical Co., St. Louis, MO.

For the stability evaluation of **1**, a solution (1 mg/mL) of pure **1** in hexane and $CHCl_3$ was prepared and monitored for 45 days by GC-MS. Additionally, samples of **1** at a concentration of 1.6 mg/ml were prepared and stored in deuterated solvents such as MeOH-d_3, $CDCl_3$, DMSO-d_6, and hexane-d_{14} in order to be monitored by qHNMR. All samples were stored at −30 °C.

Artificial degradation was induced by transferring **1** in the dry (solid) state. This was facilitated under a stream of argon, and samples (1.1 mg each) were then stored in the dark at 4 °C for 3, 6, 9, 12,18, 24, 29, 36, and 42 h, respectively, before being redissolved in 1 mL of $CHCl_3$ or 600 μL of $CDCl_3$ to undergo immediate GC-MS and qHNMR analysis.

Plant Material. Dried root material of *A. sinensis* (OLIV.) DIELS (Apiaceae) was purchased from Kiu Shun Trading Ltd., Vancouver, Canada, in 2000. The plant material was then identified by using a series of comparative macroscopic, microscopic, TLC, HPLC, and PCR analysis with Dang Gui reference plant materials obtained from the National Institute for the Control of Pharmaceutical and Biological Products of China, Beijing, People's Republic of China (lot # 927-200110). A voucher sample was deposited at the UIC/NIH Center for Botanical Dietary Supplements Research (BC165), Chicago, IL.

Summary of Extraction and Isolation. Immediately after the supercritical fluid extraction, upper and lower phases were added to the crude supercritical fluid extract. This solution was then directly applied to FCPC fractionation. Fractions were collected every 5 mL and analyzed by TLC developed in $CHCl_3$. According to their TLC profile, fractions were recombined and analyzed by GC-MS and ^{1}H NMR to furnish crude fractions of **1** and **2**. Further purification of **1** and **2** was achieved by applying selected fractions to a consecutive HSCCC experiment under the same conditions. The collected fractions (1.5 mL each) were analyzed by TLC and then recombined and analyzed by GC-MS and ^{1}H NMR. Purified **1** was kept in upper phase solution and stored at −30 °C, as these conditions were determined to be the optimal storing conditions.

***Z*-Ligustilide (1):** colorless oil; ^{1}H NMR ($CDCl_3$, 400 MHz) δ 0.960 (3H, t, J = 7.4, H-11), 1.508 (2H, tq, J = 7.4, 7.4 H-10), 2.382 (2H, dt, J = 7.4, 6.1, H-9), 2.467 (2H, pseudo ddd, J = 9.9, 4.3, 2.1, 1.5, H-5), 2.600 (2H, pseudo dt, J = 9.8, 1.8, H-4), 5.218 (1H, t, J = 8.0, H-8), 6.005 (1H, dt, J = 9.6, 4.2 H-6), 6.296 (2H, dt, J = 9.6, 2.0, H-7); ^{13}C NMR ($CDCl_3$, 400 MHz) δ 13.43 (CH_3, C-11), 18.18 (CH_2, C-4), 22.04 (CH_2, C-5/10), 28.15 (CH_2, C-9), 112.55 (CH, C-8), 116.78 (CH, C-7), 123.65 (C-7a), 129.50 (CH, C-6), 146.68 (C, C-3a), 148.20 (C, C-3), 167.28 (C, C-1); EIMS m/z (int.) 190 [M^+] (28), 161 (50), 148 (48), 134 (14), 120 (10), 115 (11), 106 (36), 105 (57), 91 (20), 79 (20), 78 (50), 77 (53), 55 (100.0), 53 (12), 51 (24); spectroscopic data consistent with previous reports.[1,18]

***Z*-Butylidenephthalide (2):** colorless oil; ^{1}H NMR ($CDCl_3$, 400 MHz) δ 0.995 (3H, t, J = 7.4, H-11), 1.561 (2H, tq, J = 7.3, 7.3, H-10), 2.465 (2H, dt, J = 7.8, 7.2 H-9), 5.642 (1H, t, J = 8.0, H-8), 7.509 (1H, ddd, J = 7.7, 7.3, 0.9, H-6), 7.661 (1H, ddd, J = 7.8, 0.9, 0.8, H-4), 7.680 (1H, ddd, J = 7.8, 7.3, 1.0, H-5), 7.895 (1H, ddd, J = 7.8, 1.0, 0.9, H-7); ^{13}C NMR ($CDCl_3$, 400 MHz) δ 13.88 (CH_3, C-11), 22.56 (CH_2, C-10), 27.82 (CH_2, C-9), 109.54 (CH, C8), 119.54 (CH, C-4), 125.29 (CH, C-7), 129.36 (CH, C-6), 134.24 (CH, C-5), 139.61 (C, C-3a), 145.41 (C, C-3), 167.40 (C, C-1); EIMS m/z (int.) 188 [M^+] (17), 160 (12), 159 (100), 146 (35), 131 (22), 115 (12), 115 (12), 105 (12), 104 (27), 103 (39), 77 (51), 76 (49), 75 (12), 55 (23), 51 (13), 50 (14); spectroscopic data consistent with previous reports.[1,18]

3,8-Epoxyligustilide (4): EIMS m/z 206 [M^+] (17.0), 177 (12), 164 (30), 136 (23), 135 (75), 122 (34), 107 (32), 91 (21), 79 (18), 77 (34), 66 (35), 65 (23), 63 (15), 55 (100.0), 53 (16), 51 (18).

Senkyunolide D (7): EIMS m/z 222 [M^+] (17.6), 193 (12), 163 (11), 136 (23), 136 (21.7), 121 (11.1), 110 (14), 109 (19), 95 (17), 92 (15), 91 (14), 82 (14), 81 (25.9), 79 (14), 77 (27.2), 67 (14) 66 (11), 55 (100), 53 (62) 51 (28); consistent with previous reports.[1,18]

4,5-Dihydro-1,3-isobenzofurandione (8): GC-EIMS m/z 150 [M^+] (17), 106 (50), 105 (54), 79 (14), 78 (100), 77 (31), 63 (32), 52 (22), 51 (40), 50 (34).

Phthalic acid anhydride (10): white, amorphous powder (reference substance); ^{1}H NMR ($CDCl_3$, 400 MHz): δ 8.033 (AA′XX, 2H, J = 7.8, 2.1, 0.8), 7.919 (AA′XX′ 2H, J = 7.8, 2.1, 0.8); EIMS m/z 148 [M^+] (17.0), 104 (100.0), 77 (17.4), 76 (95.7), 75 (16.4), 74 (31.2), 50 (48.5); spectroscopic data consistent with literature.[28]

Acknowledgment. Research was supported by grant number P50 AT00155 from the National Center for Complementary and Alternative Medicine (NCCAM) and the Office of Dietary Supplements (ODS).

The contents are solely the responsibility of the authors and do not necessarily represent official views of NCCAM or ODS.

References and Notes

(1) Deng, S.; Chen, S.; Yao, P.; Nikolic, D.; van Breeman, R. B.; Bolton, J. L.; Fong, H. H. S.; Farnsworth, N. R.; Pauli, G. F. *J. Nat. Prod* **2006**, *69*, 536–541.
(2) Sheu, S. J.; Ho, Y. S.; Chen, Y. P.; Hsu, H. Y. *Planta Med.* **1987**, *53*, 377–378.
(3) Li, P.; Li, S. P.; Lao, S. C.; Fu, C. M.; Kan, K. K. W.; Wang, Y. T. *J. Pharm. Biomed. Anal.* **2006**, *40*, 1073–1079.
(4) Lager, E.; Sundin, A.; Toscano, R. A.; Delgado, G.; Sterner, O. *Tetrahedron Lett.* **2007**, *48*, 4215–4218.
(5) Cao, Y.-X.; Zhang, W.; He, J.-Y.; He, L.-C.; Xu, C.-B. *Vasc. Pharmacol.* **2006**, *45*, 171–176.
(6) Liang, M.-J.; He, L.-C.; Yang, G.-D. *Life Sci.* **2005**, *78*, 128–133.
(7) Luo, Y.; Pan, J.; Ding, K.; Yan, Z. *Zhongcaoyao* **1996**, *27*, 456–457.
(8) Kimura, M.; Harada, M.; Sekida, S.; Yuda, M. *Pharmaceuticals containing butylidenephthalide, senkyunolide, or ligustilide for treatment of arteriosclerosis*; Tsumura and Co. Japan; National Institute of Hygiene: Japan, 1989.
(9) Nitz, S.; Spraul, M. H.; Drawert, F.; Spraul, M. *J. Agric. Food Chem.* **1992**, *40*, 1038–1040.
(10) Zhang, D.; Teng, H.; Li, G.; Liu, K.; Su, Z. *Sep. Sci. Technol.* **2006**, *41*, 3397–3408.
(11) Quiroz-Garcia, B.; Figueroa, R.; Cogordan, J. A.; Delgado, G. *Tetrahedron Lett.* **2005**, *46*, 3003–3006.
(12) Cui, F.; Feng, L.; Hu, J. *Drug Dev. Ind. Pharm.* **2006**, *32*, 747–755.
(13) Zhou, C.; Li, X. *Acta Pharm. Sin.* **2001**, *36*, 793–795.
(14) Friesen, J. B.; Pauli, G. F. *J. Liq. Chromatogr. Relat. Technol.* **2005**, *28*, 2877–2808.
(15) Friesen, J. B.; Pauli, G. F. *J. Agric. Food Chem.* **2008**, *56*, 19–28.
(16) Inui, T.; Case, R.; Chou, E.; Soejarto, D.; Fong, H.; Franzblau, S.; Smith, D.; Pauli, G. F. *J. Liq. Chromatogr. Relat. Technol.* **2005**, *28*, 2017–2028.
(17) AdamsR. P. *Identification of essential oil components by gas chromatography/mass spectrometry*; Allured Publishing Corporation: Carol Stream, Illinois, 1995.
(18) Deng, S. Phytochemical Investigation of Bioactive Constituents from Angelica sinensis. Ph.D. Dissertation, University of Illinois at Chicago, Chicago, 2005.
(19) Fischer, F. C.; Gijbels, M. J. M. *Planta Med.* **1987**, *53*, 77–80.
(20) Pauli, G. F.; Jaki, B. U.; Lankin, D. C.; Walter, J. A.; Burton, I. W. Quantitative NMR (qNMR) of Bioactive Natural Products. In *Bioactive Natural Products: Detection, Isolation and Structural Determination*, 2nd ed.; Colegate, S. M., Molyneux, R. J., Eds.; Taylor & Francis: New York, 2007.
(21) Pauli, G. F.; Jaki, B.; Lankin, D. *J. Nat. Prod.* **2007**, *70*, 589–595.
(22) Pauli, G. F.; Jaki, B.; Lankin, D. *J. Nat. Prod.* **2005**, *68*, 133–149.
(23) Pauli, G. F.; Pro, S.; Friesen, J. B. J. Nat. Prod. **2008**, *71*, 1489−1508.
(24) Dodds, E. D.; McCoy, M. R.; Rea, L. D.; Kennish, J. M. *Eur. J. Lipid Sci. Technol.* **2005**, *107*, 560–564.
(25) Wang, F. C.-Y.; Qian, K.; Green, L. A. *Anal. Chem.* **2005**, *77*, 2777–2785.
(26) Lin, L.-Z.; He, X.-G.; Lian, L.-Z.; King, W.; Elliott, J. *J. Chromatogr. A* **1998**, *810*, 71–79.
(27) Moody, J. D.; Heinze, T. M.; Cerniglia, C. E. *Biocatal. Biotransform.* **2001**, *19*, 155–161.
(28) Itoh, K.; Kiade, Y.; Yatome, C. *Bull. Environ. Contam. Toxicol.* **1998**, *60*, 786–990.
(29) Kaouadji, M.; De Pachtere, F.; Pouget, C.; Chulia, A. J.; Lavaitte, S. *J. Nat. Prod.* **1986**, *49*, 872–877.
(30) Kobayashi, M.; Fujita, M.; Mitsuhashi, H. *Chem. Pharm. Bull.* **1984**, *32*, 3770–3773.
(31) Beck, J. J.; Stermitz, F. R. *J. Nat. Prod.* **1995**, *58*, 1047–1055.
(32) Saito, T.; Hayamizu, K.; Yanagisawa, M.; Yamamoto, O.; Wasada, N.; Someno, N.; Kinugasa, S.; Tanabe, K.; Tamura, T.; Hiraishi, J. Spectral Database for Organic Compounds (SDBS). http://riodb01.ibase.aist.go.jp/sdbs/cgi-bin/cre_index.cgi?lang=eng (accessed Jan 4, 2008).
(33) Banerjee, S. K.; Gupta, B. D.; Sheldrick, W. S.; Hoefle, G. *Liebigs Ann. Chem.* **1982**, *699*, 707.
(34) Lu, G.-H.; Chan, K.; Chan, C.-L.; Leung, K.; Jiang, Z.-H.; Zhao, Z.-Z. *J. Chromatogr. A* **2004**, *1046*, 101–107.
(35) Dietz, B.; Liu, D.; Hagos, G. K.; Schinkovitz, A.; Edirisinghe, P. D.; Deng, S.; Yao, P.; Farnsworth, N. R.; Pauli, G. F.; van Breemen, R. B.; Bolton, J. L *Chem. Res. Toxicol.* **2008**, DOI: 10.1021/tx8001274.
(36) Yan, R.; Ko, N. L.; Li, S. L.; Tam, Y. K.; Lin, G. *Drug Metab. Dispos.* **2008**, *36*, 400–408.
(37) Li, G.; Ma, C.; Li, X.; Lui, K. *Chin. Trad. Herb. Drugs* **2000**, *31*, 405–407.
(38) Chen, S.-N.; Turner, A.; Jaki, B.; Nikolic, D.; van Breemen, R. B.; Friesen, J. B.; Pauli, G. F. *J. Pharm. Biomed. Anal.* **2008**, *46*, 692–698.

NP800137N